Wireless Sensor Technologies for Monitoring Civil Structures

David Mascareñas, Eric Flynn and **Michael Todd,** University of California San Diego, California
Gyuhae Park and **Charles Farrar,** Los Alamos National Laboratory, Los Alamos, New Mexico

Wireless sensor networks (WSNs) for structural health monitoring (SHM) applications can allow for a rapid assessment of structural integrity after an event such as a natural disaster puts the reliability of civil infrastructure in question. Unfortunately, there are many technical challenges associated with employing such a WSN in civil infrastructure for operation over multiple decades. Maintenance costs must remain low enough to justify the integration of such a WSN into a given structure. The technical challenges include ensuring power is delivered to the sensor nodes, reducing installation and maintenance costs, and automating the collection and analysis of data collected by a wireless sensor network. Here we explore possible solutions to the technical challenges presented by WSN for SHM applications. A "mobile host" WSN has been developed where a civil structure is instrumented with sensor nodes capable of being powered solely on energy transmitted to the sensor node wirelessly by the mobile host. When the sensor node has received adequate energy for making a given measurement, the sensor node performs the necessary measurement operations and then wirelessly transmits the measurement to the mobile host. These operations are then repeated for all desired sensor nodes in the network.

In crisis situations such as an earthquake, it is good to have tools in place allowing a rapid condition assessment of civil infrastructures. Often these situations do not allow conventional human inspections due to safety and accessibility issues. It would be desirable to automate the inspection process so that humans are not placed in danger during the assessment and to employ relevant data collection and feature extraction methods to eliminate the need for infrastructure assessment experts at a potentially damaged location.

Furthermore, this rapid assessment-monitoring system should be robust enough to be deployed on a structure for multiple decades without any human intervention. The work presented here proposes sensors and nodes that can be integrated into such a rapid assessment-monitoring framework. The sensor nodes investigated here are designed to be placed into a "roving-host," wireless-sensor network. In this framework an unmanned aerial vehicle (UAV) is used to fly to the sensors of interest. Once the UAV arrives at the relevant sensor node, it wirelessly transmits energy to the sensor node to power it up in a manner similar to the operation of a radio frequency identification (RFID) tag. The sensor node makes a measurement and then transmits data back to the UAV. The UAV then adds the sensor node's data to its database and repeats the process for other relevant nodes. Such a network allows for periodic energy delivery as well as a centralized data processing capability that can perform feature extraction on data from multiple nodes, including the SHiMmer node developed by Musiani *et al.*[1] The "roving-host" architecture is very well suited for such structural health monitoring applications.

Figure 1 shows a summary of the "roving-host" wireless sensor network developed in this test. In the scenario under consideration, an overpass is outfitted with peak displacement sensor nodes made to be powered from energy wirelessly delivered to them via microwaves. A microwave source is placed on a radio control helicopter so energy can be delivered to the node on an as-needed basis. The helicopter also features an on-board computer with a Zigbee radio and 802.11g wireless card for receiving data transmitted by the base station and sensor node. The computer is meant to be able to collect data from the sensor node and store it for future use. In a wide-scale sensor network, the helicopter would fly throughout the sensor network and collect data from every sensor of interest. The helicopter would serve as a central data repository and central data processing node for the sensor network. This work will focus on the first implementation of the "roving-host" wireless sensor network. More information on the sensor and sensor node can be found in Reference 2.

Peak Displacement Sensor Node

The wireless sensor node developed in this work is known as THINNER (Figure 2) which is made up of an ATmega128L microcontroller, an AD7745 capacitance-to-digital converter, and an XBee radio. THINNER is unique among wireless sensor nodes in three key ways. First, it was designed to be powered by wirelessly delivered energy supplied from a UAV. To operate from such a low energy source, the components were carefully selected to ensure that they would perform satisfactorily at low energy levels (<1 J). Second, THINNER employs a capacitance-to-digital converter instead of a conventional analog-to-digital converter used in most wireless sensor nodes. The capacitance-to-digital converter choice was driven by the need to store peak displacement values even in the absence of a power supply. To save this data, the sensors employed with THINNER are built so that the peak data are stored mechanically as opposed to electronically. Capacitive sensors were best suited to this type of requirement. (See more on sensors in Reference 2.) Finally, THINNER uses an XBee radio to communicate with other sensor nodes, as well as to communicate with the UAV. The XBee radio is a form of Zigbee radio developed by Maxstream. The radio interfaces with the microcontroller via a UART connection that employs standard serial port communications protocols.

RF Power Delivery

Wireless energy delivery is not a new concept. Reference 3 gives a good historical overview on research in the delivery of wireless energy. An outline of the theory used to describe wireless energy transmission by electromagnetic waves is found in Reference 4. A short description on the theory of the delivery of wireless energy is given here. In this work, radio frequency (RF) energy was typically transmitted at 2.5 GHz. This band was chosen as the transmission frequency for a variety of reasons, including the ease of obtaining inexpensive hardware at this frequency and the ability to buy high-gain antennas with a weight and volume appropriate for the radio-controled (RC) helicopter. The Friis formula can be used to describe the RF energy transmission:

$$P_R = \frac{G_T G_R \lambda^2}{(4\pi R)^2} P_T \tag{1}$$

In this equation P_R is the power received; G_T is the gain of the transmitter antenna; G_R is the gain of the receiver antenna; λ is the wavelength of the radiation; R is the distance, and P_T is the power transmitted.

The wavelength is given by:

$$\lambda = \frac{c}{f} \tag{2}$$

In this expression, c is the speed of light, and f is the frequency of the single-tone signal. The typical Friis-link parameters used in this investigation are shown in Figure 3.

Based on a paper presented at IMAC XXVI, the 26th International Modal Analysis Conference, Orlando, FL, February 2008.

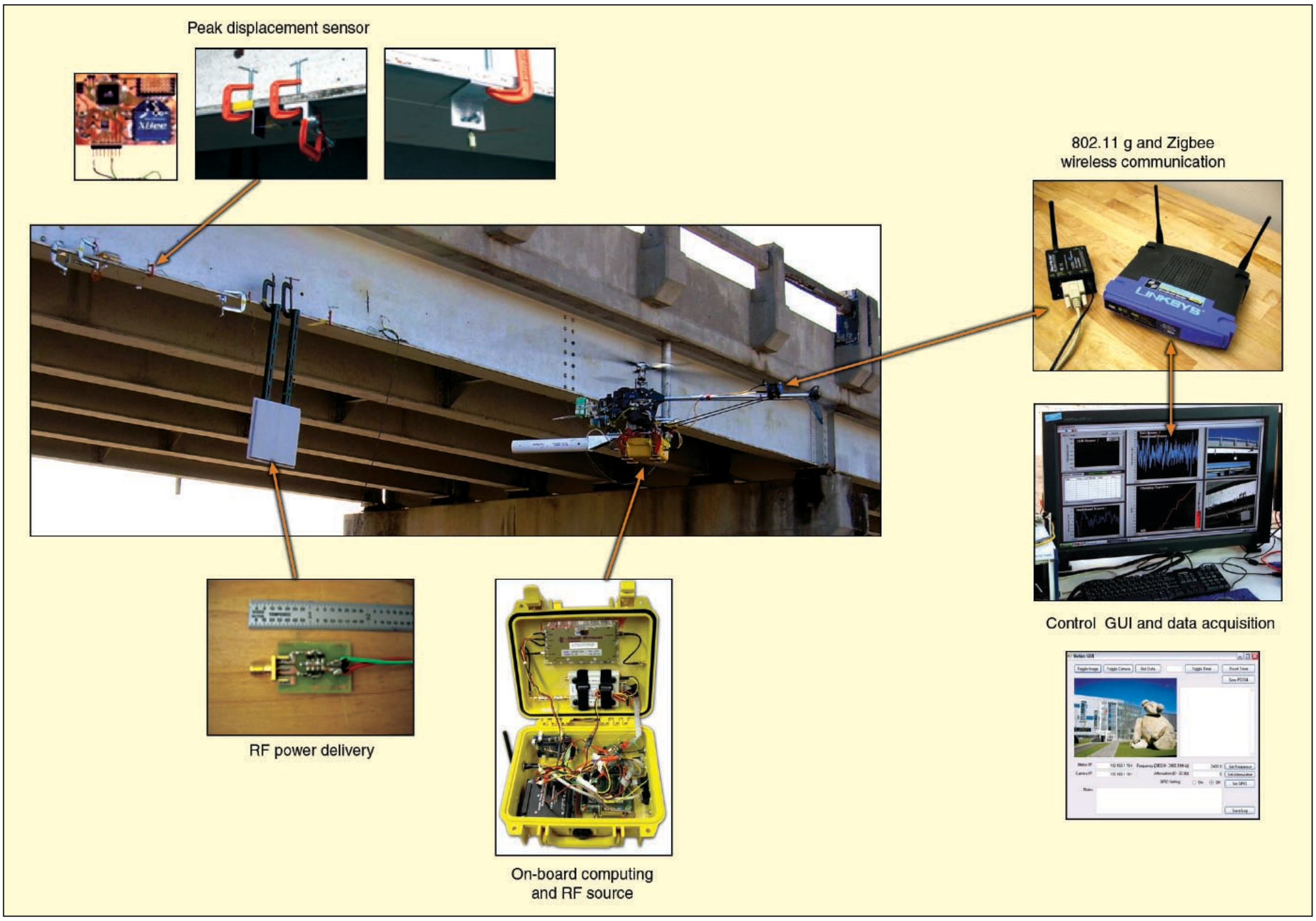

Figure 1. Summary of components used for the "roving host" wireless sensor network.

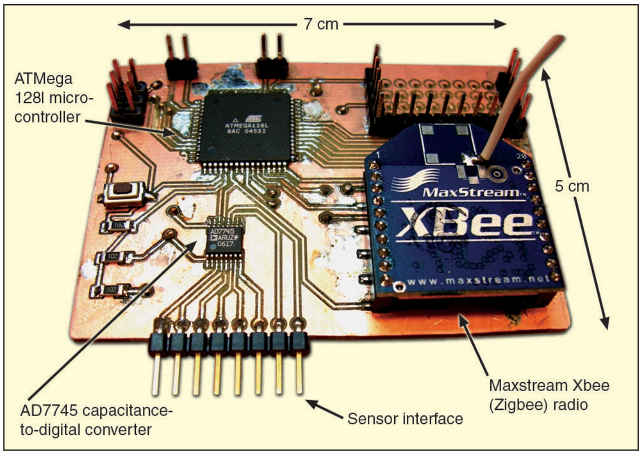

Figure 2. THINNER wireless sensor node.

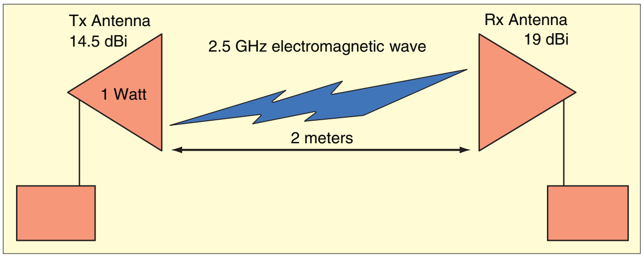

Figure 3. Typical wireless energy transmission parameters and test setup used in this investigation.

The Tx antenna is a 14.5-dBi Yagi antenna, and the Rx antenna is a 19-dBi patch antenna. The 2-meter spacing was selected as an estimated powering distance, because it appeared to be the reasonable limit of proximity the helicopter would be able to approach a bridge for the field demonstration in southern New Mexico. The values in Figure 3 can be used with Equations 1 and 2 to estimate the theoretical power delivery to the sensor node assuming 100% efficiency.

$$\lambda = \frac{c}{f} = \frac{3 * 10^8 \, m/s}{2.5 * 10^9 \, Hz} = 0.12m \tag{3}$$

$$P_R = \frac{(28.18)(79.43)(0.12m)^2}{\left(4\pi(2m)\right)^2} 1W = 0.051W \tag{4}$$

So the maximum amount of power that can theoretically be received at the Rx antenna is 51 mW. When the power is received at the antenna, it then passes through the rectification circuitry to supply a DC voltage to charge up a 0.1 Farad super capacitor. Ultimately, we decided to charge the capacitor up to 3.5 V. With this information, we can calculate the energy in the capacitor as well as the lowest possible time to charge the capacitor. Equation 5 gives the expression for calculating the energy in a capacitor:

$$E = \frac{1}{2} C V^2 \tag{5}$$

In this expression, E is the energy, C is the capacitance and V is the voltage. Inserting the relevant information yields:

$$E = \frac{1}{2}(0.1F)(3.5V)^2 = 0.6125 Joules \tag{6}$$

$$Time = \frac{E}{P_R} = \frac{0.6125 Joules}{0.051W} = 12.0 \sec \tag{7}$$

So for the assumed 2-meter distance, the capacitor can be charged up in no less than 12 seconds, assuming there are no losses due to the rectifier, antennas, destructive interference, misalignment errors, positioning errors, etc.

UAV On-Board Computing

Computing on the helicopter is provided by an AMD Geode

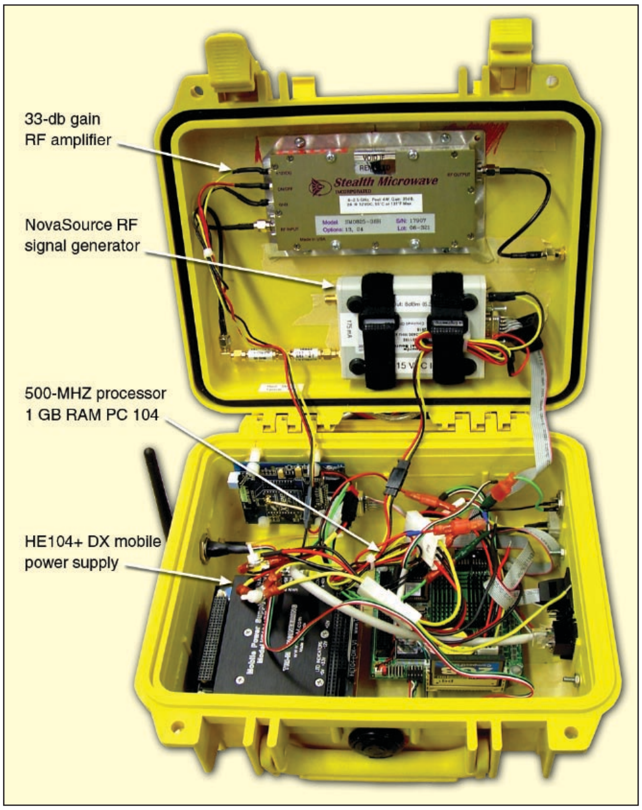

Figure 4. Helicopter payload.

LX 800 CPU running Unbuntu Linux. The computer boots from a compact-flash card for weight savings and to eliminate moving parts within the helicopter payload that might compromise reliability. The CPU controls a NovaSource RF signal generator via an RS-232 connection. The RF source sends signals into the RF amplifier so the power level is suitably high for wireless power delivery (~1 Watt). The computer is running Apache web server, allowing command and control of the computer and RF source from the base station via 802.11g. Data are received from the sensor node via an RS-232 enabled XBee modem. The data are stored in the helicopter memory until requested by the base station. Figure 4 shows the helicopter on-board computing package.

X-Cell Spectra G Helicopter

The helicopter airframe used in this test is the X-Cell Spectra G. The helicopter power plant is a 23-cc, two-cycle gas engine. The helicopter is using 810-mm anti-symmetrical, high-lift blades to carry the computational and RF payload. In addition the stock exhaust was exchanged for a Hatori muffler, enabling a broadened power curve. The helicopter weighs approximately 12 lb ready to fly in the stock condition. When loaded with the sensor network payload, the total weight of the helicopter rose to ~22 lb. In the fully loaded condition, the 8 oz fuel tank provided approximately 5 to 6 minutes of run time at 5300 ft, 90° F and calm winds. Flight duration was generally hampered by either the engine overheating and losing power, or the helicopter running out of fuel. The helicopter is also carrying an Axis 207W wireless webcam for recording events as seen by the helicopter. Figure 5 shows the various components on the helicopter.

Alamosa Canyon Bridge Field Test

To demonstrate the capabilities of the mobile host in real-world conditions, a field test was conducted on the Alamos Canyon Bridge in southern New Mexico. This bridge was decommissioned by the New Mexico Department of Transportation and is made available to researchers for testing new structural monitoring technologies. The bridge is 24 ft wide and consists of seven 50-ft spans that are approximately 15 ft above a ravine. Sensors were mounted at the bottom of one of the steel beams supporting the concrete deck of the middle span. A base station and helipad were set up in the riverbed approximately 30 ft from the instrumented span. Figure 6 shows the bridge (a) and base station (b). During this test, the capacitive sensors were tested against traditional gages, and the RF charging and data retrieval scheme were demonstrated using the RC helicopter.

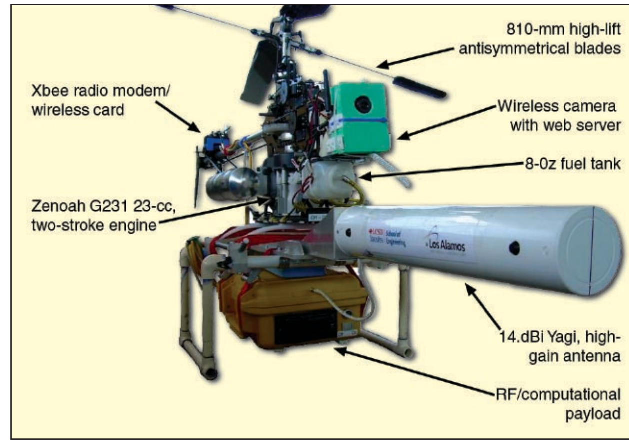

Figure 5. "Roving-host" wireless sensor node.

Figure 6. Alamosa Canyon Bridge test setup.

Interrogator Base Station

A research-oriented base station (Figure 7) was developed for the test at Alamosa Canyon. This base station served as both a communication link with the mobile host as well as a data acquisition system for collecting comparative measurements using traditional wired sensors. The backbone consists of a National Instruments (NI) PXI chassis combined with a built-in computer and NI LabView software. A custom-built virtual instrument developed in LabView acquired, conditioned, displayed, and logged data transmitted by the capacitive sensors, the traditional sensor gages, and the on- and off-board wireless video cameras (Figure 8). The software also tracked the voltage across the super capacitor used to power the

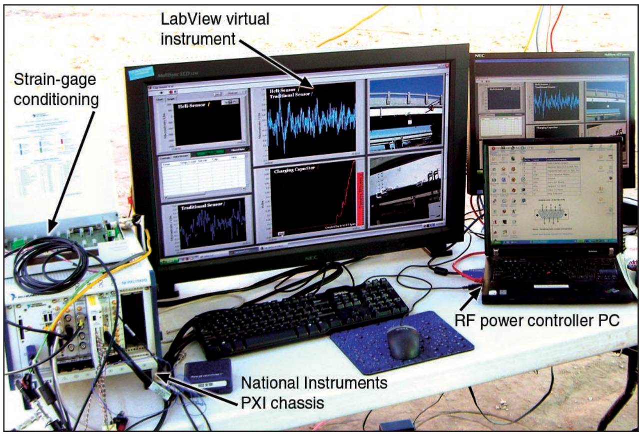

Figure 7. Base station.

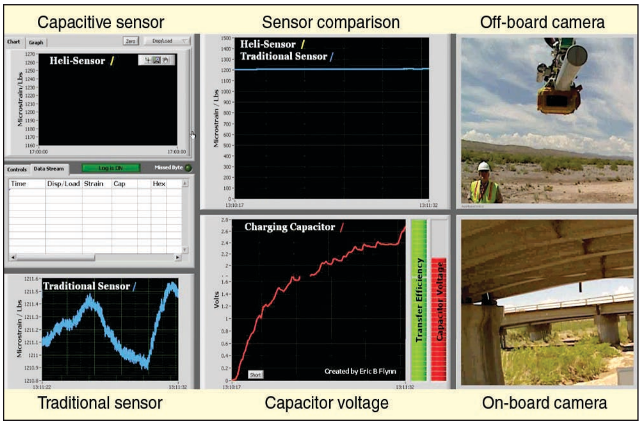

Figure 8. Data Acquisition GUI.

sensor as well as the RF power transfer efficiency. Additionally, a graphical user interface developed in C# was used to control the on/off state and frequency of the RF power transmitter on the mobile host.

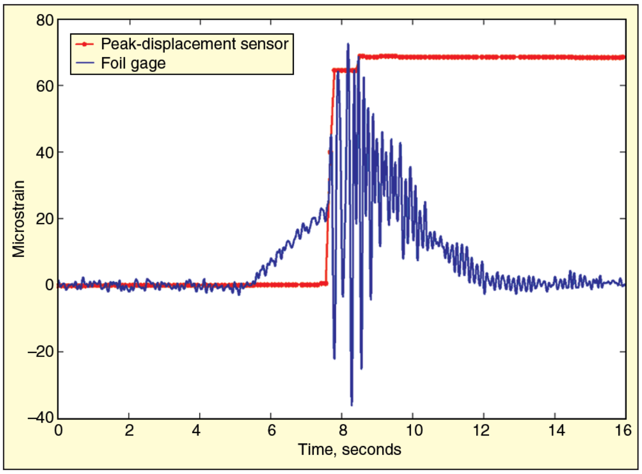

Figure 9. Peak displacement sensor vs conventional foil strain gage.

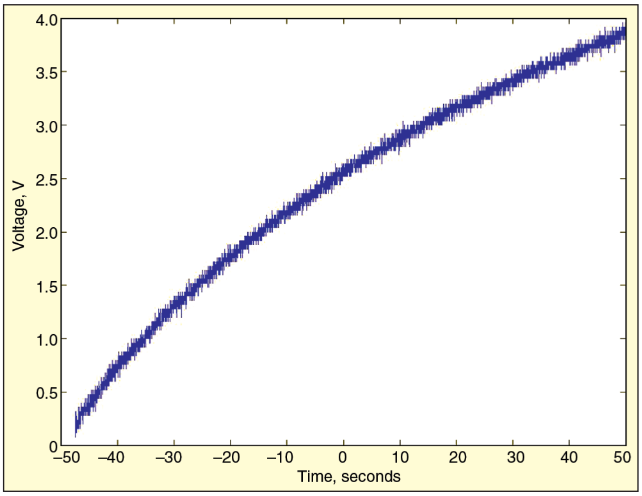

Figure 10. Voltage on 0.1-F capacitor when connected to full-wave voltage quadrupler.

Peak Displacement Sensor / Strain Gage Comparison

Using the base station for acquisition, a verification of the capacitive peak displacement was performed. The peak displacement sensor was collocated with a traditional foil strain gage at the center of one of the bridge spans. The sensor was attached to a battery for continuous streaming of measurements. These streaming measurements, along with the dynamic strain readings, were collected in LabView. Dynamic excitation was provided by a 22-ton dump truck driven over a piece of 2 × 4 lumber placed across the road at the center of the span. Figure 9 shows the reading from the foil strain gage and the peak displacement sensor (calibrated to the equivalent strain measurement). As anticipated, the peak sensor held the maximum positive experienced strain even after the bridge returned to the original unstrained state. The small discrepancy in timing and amplitude was attributed to the low-pass filtering in the conditioning circuit of the foil strain gage and inaccuracies in the calibration of the peak displacement sensor.

RF Charging and Data Retrieval

Experimental evaluation of the RF energy delivery circuit consisted of two different tests. The first experiment involved using the RF energy delivery setup in the laboratory environment. The second test involved use of the RF energy delivery to charge up a THINNER sensor node on the bridge. A summary of the results from the three tests follows.

RF Energy Delivery in Lab

The first tests conducted using the RF energy delivery were done at CALIT^2 in San Diego and at the Los Alamos National Labs Engineering Institute. The RF energy delivery hardware was set up as noted in the theoretical section above. A full-wave voltage quadrupler was used as the RF-to-DC converter. The results of these tests are presented in Figures 10 and 11. The tests showed that the typical time for the 0.1-F capacitor to charge to 3.5 V was 95 seconds. If we define the average power as the slope of a least-squares fit to the calculated energy on the 0.1-F capacitor, the average power delivered is 8.1 mW. This value was deemed acceptable for the first version of the "mobile-host" wireless sensor node. Next, the RF energy delivery was tested on the bridge at Alamosa Canyon.

RF Energy in the Field

The first full-scale test of the "mobile-host" wireless sensor node was at the Alamosa Canyon Bridge. The THINNER sensor node was placed on the understructure of the bridge. A capacitive peak displacement sensor was connected to THINNER. The 19-dBi antenna was hung slightly below the longitudinal steel bridge supports. The RF energy delivery equipment was placed on an RC Spectra G helicopter, which was manually flown up to the 19 dBi patch antenna on the bridge to charge up the THINNER sensor node. An image of the Alamosa Canyon Bridge test setup is shown in Figure 12.

A plot showing the charging characteristics of the THINNER sensor node due to the RF energy delivery of the helicopter is shown in Figure 13. Figure 14 shows the calculated energy on the 0.1-F capacitor as it is charged. From these plots, we see that to reach 3.5 volts took more than 270 seconds, which is significantly longer than the 95 seconds needed in the laboratory experiment. The reason for this discrepancy can be attributed to a few different factors. First, the pilot reported that the helicopter was very difficult to align with the patch antenna on the bridge for two reasons. The first reason was that the pilot was on the ground level, and he did

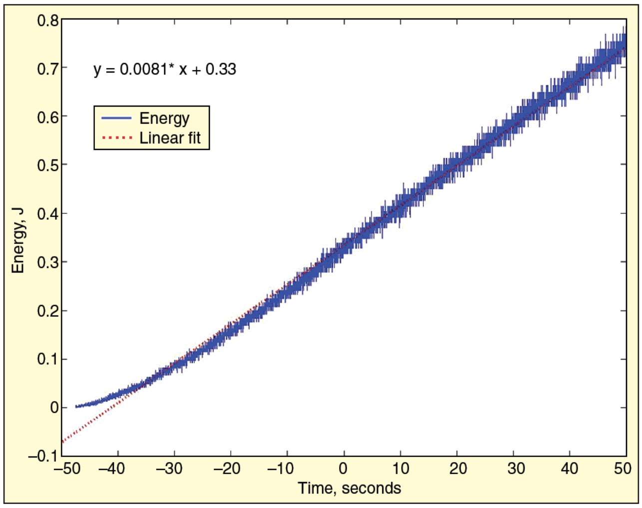

Figure 11. Energy in 0.1-F capacitor connected to full-wave voltage quadrupler. Note the power is 8.1 mW.

Figure 12. Alamosa Canyon Bridge test setup.

not have a good view of the alignment between the patch antenna and the Yagi antenna. The pilot had very little feedback as to the quality of RF link he was maintaining. The second major problem was that the wind blowing under the bridge was making antenna alignment difficult. In addition, the pilot also reported a tendency for the helicopter to want to travel into the bridge, so he would need to periodically draw back from the bridge structure to avoid damage to the helicopter. Video footage of the tests shows that the helicopter is constantly traveling in a loop in an effort to maintain the proper distance and orientation of the bridge. This behavior is also observed in the voltage vs. time plot (Figure 13).

The plot exhibits characteristics in common with a stair step. The flat portions of the stairs correspond to times when the helicopter was either too far away from the antenna or was misaligned with the patch antenna. The vertical portions of the stairs correspond to the periods when the helicopter was tending to move toward the bridge or had the best alignment with the patch antenna. If we once again take an average of the power delivery in a least-squares sense (Figure 14), we have an estimated average power delivery of 2.5 mW. The value of the power delivered in the field is significantly lower than the power delivered in the lab. The discrepancy is mainly due to errors associated with the misalignment of the antennas. One interesting feature of Figure 14 is that there is a portion between 166 and 180 seconds where there is a higher power delivery over a characteristically significant time than most of the rest of the plot. Despite the low-power RF energy delivery, the THINNER sensor node was successfully charged to 3.5 V, and the sensor node completed three peak displacement sensor measurements with the energy stored in the 0.1-F capacitor.

Conclusions

A "roving-host," wireless sensor networking paradigm was proposed and tested. A commercially available radio-controlled helicopter was equipped to deliver microwave energy to wireless sensor nodes located on a decommissioned overpass in southern New Mexico. The helicopter successfully delivered sufficient microwave energy to charge a wireless sensor node to make multiple peak displacement measurements and transmit the data back to the helicopter. The results of this experiment show that a "roving-host" wireless sensor network can feasibly be used to distribute energy to sensor nodes on an as-needed basis. In future work, the "roving-host" wireless sensor network will be expanded to perform a variety of measurements relevant to structural health monitoring such as collecting data from piezoelectric sensors.

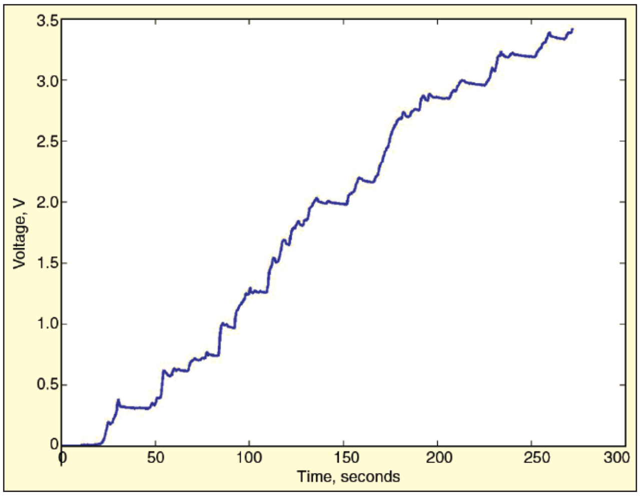

Figure 13. Voltage on 0.1-F capacitor as the helicopter charges THINNER.

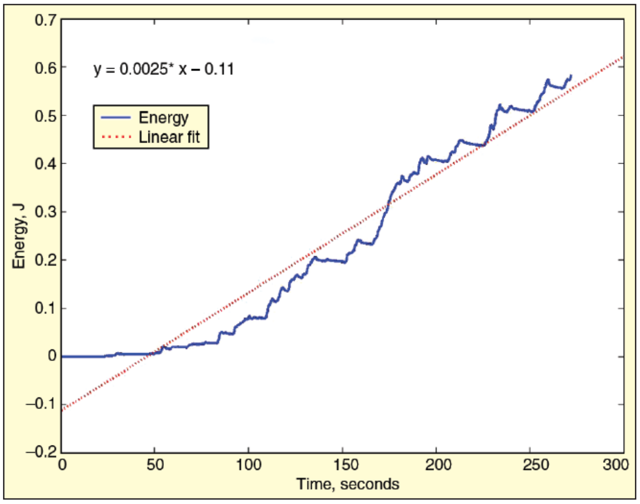

Figure 14. Calculated energy in 0.1-F capacitor as helicopter charges THINNER.

Acknowledgements

The authors would like to acknowledge the work of Kaisen Lin, Rajesh Gupta, and the New Mexico Department of Transportation, who helped make this project possible.

References

1. Musiani, D., Lin, K., Rosing, T., "An Active Sensing Platform for Structural Health Monitoring," presented at the Sixth International Symposium on Information Processing in Sensor Networks, April 25-27, 2007 Cambridge, MA.
2. Mascarenas, D., Todd, M., Park, G., Farrar, C., "A Low-Power Wireless Sensor Node for Peak Displacement and Bolted Joint Preload Measurements, *Proceedings of the 6th International Workshop on Structural Health Monitoring*, F. Chang (Ed.), Technomic, 2007
3. Brown, W.C., "The History of Power Transmission by Radio Waves," *IEEE Transactions on Microwave Theory and Techniques*, Vol. 32, No. 9, pp. 1230-1242, 1984.
4. Pozar, D., *Microwave Engineering, Third Edition*. John Wiley and Sons., pp. 647-649, 2005.

You can reach the author at: dmascare@ucsd.edu.